

Possible reordering of vortex matter near the end point of the second peak line in the $\text{YBa}_2\text{Cu}_3\text{O}_{7-\delta}$ compound

D. Stamopoulos and M. Pissas

Institute of Materials Science, NCSR, Demokritos, 153 10 Aghia Paraskevi, Athens, Greece

A. Bondarenko

Kharkov State University, 310077 Svoboda square 4, Kharkov, Ukraine

(Received 12 March 2002; revised manuscript received 26 June 2002; published 30 December 2002)

We report on the second peak line H_{sp} and the possible phases of vortex matter near T_c for a detwinned underdoped $\text{YBa}_2\text{Cu}_3\text{O}_{7-\delta}$ single crystal. Our local ac and dc permeability measurements revealed that the second peak line H_{sp} does not terminate either at the critical temperature or on the irreversibility line H_{irr} . Pronounced hysteretic behavior is observed in the regime below the second peak line H_{sp} . Below (above) a characteristic field the end point of the second peak differs from (coincides with) the irreversibility point, $H_{\text{end point}} \neq H_{\text{irr}}$ ($H_{\text{end point}} \equiv H_{\text{irr}}$). A possible reentrance of a dynamically ordered solid phase in the high-temperature regime near the irreversibility line is discussed.

DOI: 10.1103/PhysRevB.66.214521

PACS number(s): 74.60.Ge, 74.60.Jg

Despite the progress having been done in the study of the mixed vortex state in high- T_c superconductors under the presence of disorder, several issues remain unclear, from the theoretical as well as the experimental point of view.¹⁻³ Theoretical proposals, including different vortex phases such as quasilattice (Bragg glass),⁴⁻⁹ entangled glass,^{5,8-10} and liquid,¹¹⁻¹⁴ have focused the effort of experimentalists, in order the existence of a universal phase diagram to be confirmed.

One of the high- T_c superconductors widely studied experimentally is $\text{YBa}_2\text{Cu}_3\text{O}_{7-\delta}$. This particular superconductor exhibits three-dimensional behavior over all scales of the phase diagram (H, T) experimentally accessible. It is widely accepted that the oxygen deficiency (δ) in high-quality detwinned $\text{YBa}_2\text{Cu}_3\text{O}_{7-\delta}$ single crystals is responsible for the pinning of flux lines. The most pronounced consequence of lowering (increasing) the oxygen content is the movement of the fishtail line [this line is the locus of (H, T) points where the screening current displays a peak, also called second peak (SP)] to lower (higher) magnetic fields.¹⁵⁻¹⁸ For the case of nearly optimally doped crystals, in the region between the first peak line H_{fp} and the onset line H_{onset} of the second peak, when the additional effective pinning is weak, the magnetic response is controlled by the edge barrier (geometrical/surface barriers).¹⁹ In such high-quality single crystals, the SP line H_{sp} is placed to high magnetic fields, while dc magnetization measurements revealed the existence of a kink point (KP) above the onset point (OP) of the SP in the magnetization loops.²⁰⁻²³ For δ lower than 0.07 (*overdoped regime*) the SP line displays a nonmonotonic variation with temperature and is terminated near the melting line. Instead, when δ is higher than 0.07 (*underdoped regime*) different behavior has been observed. In this regime the SP line decreases monotonously as temperature increases and tends to terminate at T_c .

Today, this picture holds for high- T_c cuprates, where both experimental^{15-18,24,25} and theoretical⁴⁻⁹ works conclude that, inconsequentially of its temperature variation, the SP

line H_{sp} shifts to lower fields as the point disorder (including oxygen deficiency) increases. On the other hand, there is no experimental evidence that the OP and SP lines terminate on the melting line, as should be expected according to classical thermodynamic arguments, or stop at a characteristic point which is placed near (but not on) this first-order phase boundary. Recently, the position of the SP line and how this line terminates on the melting line, for different amounts of static disorder, were investigated theoretically.²⁶ In that work, extending previous studies that considered the order-disorder transition to occur entirely inside the single-vortex pinning regime, the possibility that the transition lies in the small or large bundle regime was also examined. Those theoretical results reproduced accurately the copious experimental data of Refs. 18, 15, and 16 for the case of rather small values of the dimensionless disorder parameter $D = \varepsilon \xi(0)/L_c(0)$. In contrast, for the case where the parameter D takes high values, it is not experimentally clear how the order-disorder line terminates on the melting line. This is so, because global experimental techniques that are usually employed for the investigation of high- T_c cuprates, have not sufficient sensitivity (low filling factor) to detect very small signals. Instead, local techniques are very sensitive (unity filling factor) due to the small active area of the Hall sensor, so they are convenient even for the investigation of very small single crystals.

To this end we performed systematic local dc and ac permeability measurements in a detwinned slightly underdoped $\text{YBa}_2\text{Cu}_3\text{O}_{7-\delta}$ single crystal. Our measurements indicate that the SP line does not terminate at the critical temperature as usually assumed for underdoped disordered single crystals. An end point of the SP line is experimentally captured at about $(H, T) \approx (200 \text{ Oe}, 91.2 \text{ K})$. In addition, a reentrance of the low-field quasiodordered vortex state in the high-temperature regime, near the irreversibility line H_{irr} , is possible. So, for an isothermal procedure, as we increase the magnetic field the vortex matter first exhibits an order-disorder crossover. For even higher fields the reverse process

(ordering of vortices) seems to take place just below the irreversibility point. Finally, we observed pronounced hysteretic behavior below the SP in our local ac permeability curves for increasing and decreasing the temperature, in agreement to recent experimental works.^{27,28}

I. EXPERIMENTAL DETAILS

The results presented in this work refer to a detwinned ($1.25 \times 1.15 \times 0.035 \text{ mm}^3$), slightly underdoped crystal. The crystal was grown with the self-flux method in a gold crucible. Thermal treatment was made at 450°C , in oxygen flow and ambient pressure. Detwinning was performed at 400°C in air under a pressure $\approx 25 \text{ MPa}$, followed by additional annealing in oxygen flow at 400°C and ambient pressure for three days. Its critical temperature is $T_c = 92.4 \text{ K}$ and the transition width under zero dc field and a small ac field ($H_0 = 0.14 \text{ Oe}$) is 0.2 K . This crystal exhibits the KP, which is in close proximity to the OP of the SP in both the increasing and decreasing branches of magnetization loop measurements.²⁰ This effect is observed only in high-quality single crystals.^{20–23} For our local magnetic induction measurements we used a $\text{Ga}_x\text{As}_{1-x}\text{In}$ Hall sensor with an active area of $50 \times 50 \mu\text{m}^2$. The ac [$H_{ac} = H_0 \sin(2\pi ft)$, $f = 10 \text{ Hz}$] and dc magnetic fields were applied parallel to the crystal's c axis ($\mathbf{H}_{dc} \parallel \mathbf{H}_{ac} \parallel c$). The local magnetic permeability has been deduced from Hall voltage, which is modulated by a low-frequency ac magnetic field superimposed to the dc one. The in-phase and out-of-phase signal has been measured by means of two lock-in amplifiers.^{25,29} Temperature stabilization was better than 20 mK . The ac permeability measurements were performed as a function of temperature (isofield measurements) and also as a function of the applied field (isothermal measurements). In addition, we performed global superconducting quantum interference device (SQUID) and local Hall dc magnetization measurements.

II. RESULTS AND DISCUSSION

Figures 1(a) and 1(b) show the temperature dependence of the real part μ' of the local ac permeability for several amplitudes of the ac field H_0 , under dc magnetic fields 450 Oe (near T_c), and 3000 Oe (from 5 K up to T_c), respectively, with field-cooled initial condition. This set of measurements revealed a number of interesting features. By inspection of Fig. 1(a) we can define four characteristic points. The first is the end point of the transition (where $\mu' = 1$), which is denoted as T_{irr} . This point corresponds to the crossing of the irreversibility line $H_{irr}(T)$ during warming for $H_{dc} = 450 \text{ Oe}$, as our global SQUID magnetization measurements confirmed (not shown here). The second point is located at the temperature where for some H_0 the μ' displays a local minimum and, as the comparison to global SQUID data revealed, corresponds to the temperature T_{sp} where the SP is equal to 450 Oe . More interestingly, we observe that the SP can be detected only in a range of the ac magnetic field. For low or high amplitudes of the ac field the SP is not distinct. The third and the fourth points are placed above and below T_{sp} . These are the end point and onset temperatures,

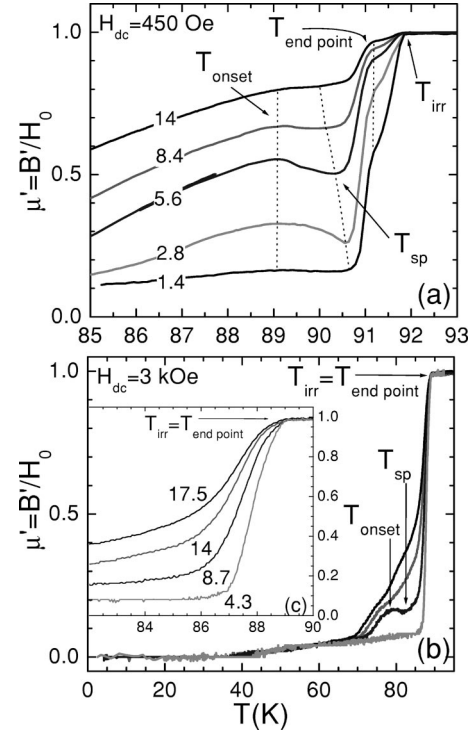


FIG. 1. Real part, $\mu' = B'/H_0$, of the local fundamental ac permeabilities as a function of temperature, for two dc fields $H_{dc} = 450 \text{ Oe}$ (a) and 3000 Oe (b) and various amplitudes of the ac field. In inset (c) we focus in the high-temperature part of the measurement, near the irreversibility point.

denoted by $T_{end\ point}$ and T_{onset} , respectively [see Fig. 1(a)]. These two points T_{onset} and $T_{end\ point}$ essentially define the temperature regime where the fishtail effect extends. One of the main results of this paper is that in the low-field regime the end point $T_{end\ point}$ differs from the irreversibility point T_{irr} as is evident in Fig. 1(a), where the dc field is $H_{dc} = 450 \text{ Oe}$. In the high-field regime the situation is rather different. Our measurements showed that for high dc fields the two points practically coincide as we observe in Figs. 1(b) and 1(c) for the case where $H_{dc} = 3000 \text{ Oe}$. At this point we must note that the global SQUID measurements in the regime near T_c are very noisy, probably because of fast relaxation, making difficult the estimate of such characteristic points from the type of measurements.

Figure 2 shows how the isothermal global moment (measured using a SQUID magnetometer) varies with external magnetic field at $T = 88 \text{ K}$ and $T = 91.2 \text{ K}$. The data at $T = 88 \text{ K}$ are compatible with an onset point and a peak in the screening current at approximately 1000 Oe and 2100 Oe , respectively. At this temperature the irreversibility field H_{irr} which is approximately 7000 Oe (as defined from the global SQUID measurement) coincides to the end point of the peak effect (as this is defined from the respective local Hall ac permeability measurement). On the other hand, the data at $T = 91.2 \text{ K}$, although do not exhibit clearly the peak effect, as the local Hall measurements show, revealed that the irreversibility field does not coincide to the end point of the peak effect (as this is defined from the respective local Hall measurement).

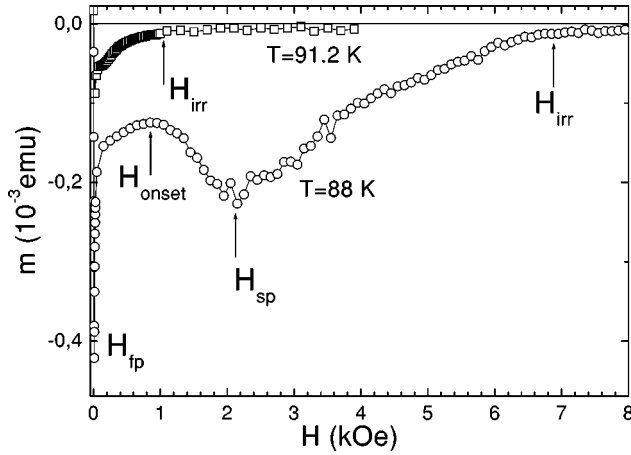


FIG. 2. Global magnetic moment as function of external magnetic field at $T=88$ K and $T=91.2$ K. The measurements are taken after zero-field cooling.

Figures 3(a) and 3(b) show in detail the variation of the real, $\mu'(T)$, and imaginary, $\mu''(T)$, parts of the local ac permeabilities as a function of temperature for various dc fields and $H_0=14$ Oe. In insets 3(c) and 3(d) we present the same measurements in an extended temperature regime.

These measurements reveal in detail that the signal possesses structure above the characteristic point $T_{\text{end point}}$. We clearly observe that the end point $T_{\text{end point}}$ of the SP does not coincide with the irreversibility point T_{irr} . In addition, we see that as we apply lower dc magnetic fields the SP is ob-

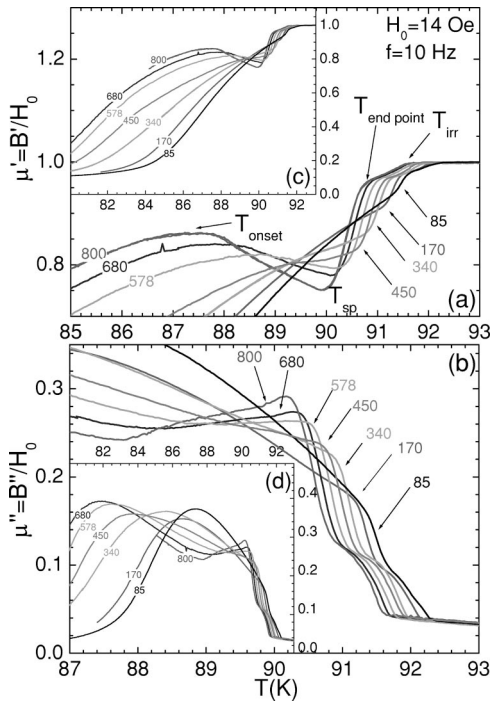


FIG. 3. Real, $\mu' = B'/H_0$ (a), and imaginary, $\mu'' = B''/H_0$ (b), parts of the local fundamental ac permeabilities as a function of temperature, for various applied dc fields in 14 Oe ac field. Insets (c) and (d) present the measured permeabilities in an extended temperature regime.

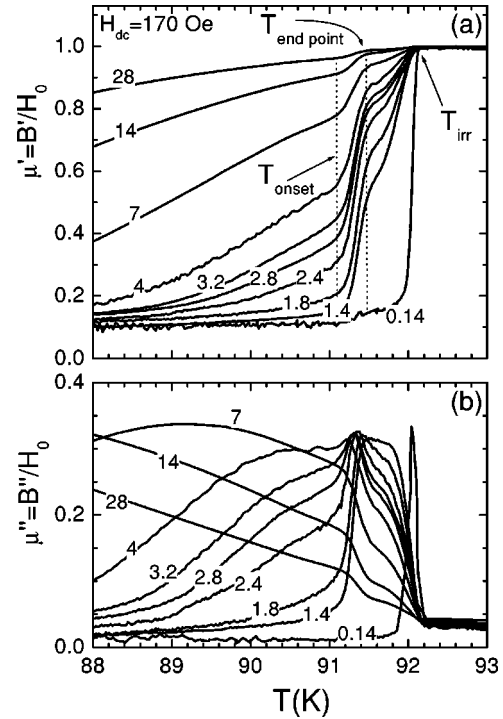


FIG. 4. Temperature variation of the real, $\mu' = B'/H_0$ (a), and imaginary, $\mu'' = B''/H_0$ (b), parts of the local permeabilities, for various ac fields and $H_{\text{dc}}=170$ Oe.

scured. For magnetic fields $H_{\text{dc}} < 500$ Oe the SP is not observed for such a high ac magnetic field, and only an abrupt change in the slope of μ' is still evident. We also performed ac permeability measurements as a function of the applied dc field and low enough amplitudes of the ac field (isothermal measurements). Those measurements revealed that the SP was present for even lower dc fields. At the end, below the characteristic point $(H, T) \approx (200 \text{ Oe}, 91.2 \text{ K})$ we were not able to detect the SP, although we examined this possibility by changing the amplitude of the ac field for two orders of magnitude.

In Figs. 4(a) and 4(b) we present the observed behavior of the real and imaginary permeabilities, respectively, for a constant dc field $H_{\text{dc}}=170$ Oe and various ac fields. We see that the SP effect is absent, even if we probe the current–electric-field $[E(J)]$ characteristics in very low (small ac field) or high (high ac field) electric-field levels. Instead of the SP, only a sharp increase in $\mu'(T)$ is observed. The characteristic temperatures T_{onset} and $T_{\text{end point}}$ where this step occurs almost do not depend on the amplitude of the ac field. A sharp drop in $J_c(T)$ similar to the one we detect at $T_{\text{end point}}$ is commonly observed for the $\text{YBa}_2\text{Cu}_3\text{O}_7$ superconductor in ac susceptibility^{30–33} or resistivity^{32,34–37} measurements. Such a sharp drop of the screening current may be accompanied by a peak effect^{31,33,36} or not^{30,32,34–37} and, as the comparison to dc magnetization measurements confirmed, is related to melting of vortex matter.^{30,31,33,37} Our measurements indicate that a similar behavior could be observed as a crossover effect of an incomplete SP in the low-field regime. Our results, in some degree confirm, and further clarify the results of previous experimental works.²⁸ We must note that

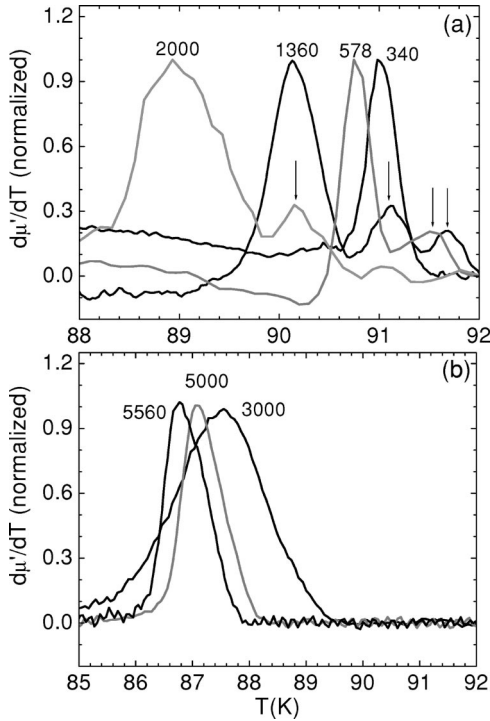


FIG. 5. Temperature variation of the derivative of the real part, $\mu' = B'/H_0$, for representative dc fields below (a) and above (b) the characteristic field $H \approx 3000$ Oe. Arrows indicate the smaller peaks placed in high temperatures.

the results presented in Ref. 28 refer to a twinned single crystal. In this work we present results for a point disordered crystal. Furthermore, in our work we promote the structure exhibited in our local measurements above the $T_{\text{end point}}$ when they were performed in the low-field regime ($H \leq 3000$ Oe). In the high-field regime ($H \geq 3000$ Oe) the signal possesses no structure indicating that the end points of the SP and the irreversibility points coincide. In order to leave no margin of doubt, in Figs. 5(a) and 5(b) we present the temperature variation of the derivative (normalized) of the real local permeability for representative dc fields below and above the characteristic point $H \approx 3000$ Oe. We see that for $H \leq 3000$ Oe, two distinct peaks are obvious, indicating that $T_{\text{end point}} \neq T_{\text{irr}}$, while for $H \geq 3000$ Oe only one peak is present, indicating that $T_{\text{end point}} \equiv T_{\text{irr}}$.

Our experimental observations for the detwinned $\text{YBa}_2\text{Cu}_3\text{O}_{7-\delta}$ single crystal are summarized in Fig. 6 where plotted is the (H, T) “phase diagram.” Depicted are the curves formed by the OP, the SP points, the end points of the SP, and the irreversibility points. All data come from local Hall measurements, except for open squares that come from global SQUID measurements. We observe that the low-field irreversibility line, coming from local measurements, is the natural consecution of the high-field part that is detected by global SQUID measurements. The irreversibility points can be fitted by the equation $H_{\text{irr}} = H_{\text{irr}}^0 (1 - T/T_c)^\nu$, where $H_{\text{irr}}^0 = 373 \pm 7$ kOe, $T_c = 92.45$ K, and $\nu = 1.34 \pm 0.05$ and is plotted in Fig. 6 by a thick solid line. We observe that the SP line H_{sp} does not terminate either at the critical temperature or on the irreversibility line H_{irr} , but could be detected until

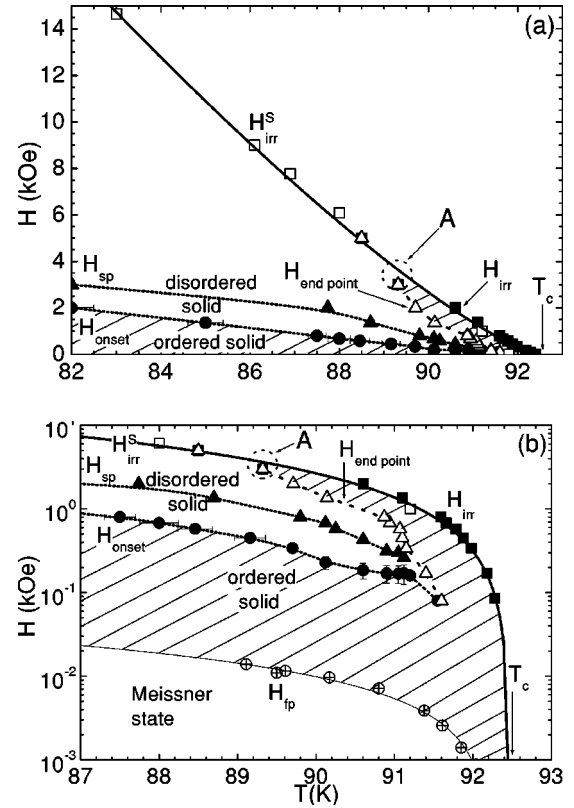


FIG. 6. The phase diagram of vortex matter in an extended regime (a) and close to the critical temperature (b). Presented are the first penetration line H_{fp} , the OP line H_{onset} (solid circles), the SP line H_{sp} (solid triangles), the end point of the second peak, $H_{\text{end point}}$ (open triangles), and the irreversibility line H_{irr} (solid and open squares coming from local Hall and global SQUID measurements, respectively). The solid line through the $(T_{\text{irr}}, H_{\text{irr}})$ points is a least-squares fitting by using the $H_{\text{irr}} = H_{\text{irr}}^0 (1 - T/T_c)^\nu$, where $H_{\text{irr}}^0 = 373 \pm 7$ kOe, $T_c = 92.45$ K, and $\nu = 1.34 \pm 0.05$. The SP line disappears at $(H, T) \approx (200 \text{ Oe}, 91.2 \text{ K})$ while the H_{onset} and $H_{\text{end point}}$ lines tend to the T_c but survive until the characteristic point $(H, T) \approx (80 \text{ Oe}, 91.6 \text{ K})$. The H_{irr} line ends at the critical temperature. The $H_{\text{end point}}$ and H_{irr} lines merge at about 3000 Oe. Dot and dashed lines are just guides to the eye.

the point $(H, T) \approx (200 \text{ Oe}, 91.2 \text{ K})$. In addition, our results show that both the onset H_{onset} and the end point $H_{\text{end point}}$ lines could not be clearly detected at very low dc fields [where only an extremely weak anomaly survives in our $\mu'(T)$ curves]. So, we conclude that, for this particular crystal, the H_{onset} and $H_{\text{end point}}$ lines tend to the critical temperature but can be detected until the point $(H, T) \approx (80 \text{ Oe}, 91.6 \text{ K})$. Furthermore, below the characteristic point $H \approx 3000$ Oe the lines $H_{\text{end point}}$ and H_{irr} are distinct ($T_{\text{end point}} \neq T_{\text{irr}}$) while for fields $H \geq 3000$ Oe they practically coincide ($T_{\text{end point}} \equiv T_{\text{irr}}$). Our results then indicate that the end point line, $H_{\text{end point}}$ may be the natural continuity of the H_{onset} line. It seems then that both lines are part of the same order-disorder line which turns around and terminates on the irreversibility line H_{irr} . This conclusion is further supported if we take into account the fact that two distinct solid phases of different degree of order should always be separated by a transition or crossover line.

Recently, Mikitik and Brandt investigated the phase diagram of vortex matter for various degrees of static disorder for the two cases of δT_c and δl pinning.²⁶ They concluded that for the case of δT_c pinning, and sufficiently strong static disorder [$D/c_L = \varepsilon \xi(0)/L_c(0)c_L > 1$], the order-disorder line decreases in the high-temperature regime, close to T_c . The new concept they introduced is that, when the transition line crosses the single-vortex pinning line (entering the regime where pinning of small/large vortex bundles takes over) it exhibits the opposite behavior and increases as approaches the melting line. Under this point of view, we could attribute the composite line, which is comprised by the H_{onset} and the $H_{\text{end point}}$ lines, to the order-disorder transition. Interestingly, the SP line H_{sp} then refers to the boundary where pinning of single vortices and bundles of vortices is distinguished.

Of course, we cannot disregard the dynamic character of our measurements and the fact that we study the excited system of vortices under the influence of the applied ac fields. Considering this, one would naturally object that the behavior observed in the high-temperature regime is not an equilibrium property of vortex matter. In the past years a lot of work is done in the subject of dynamic transitions of vortex matter when subjected to an applied driving force.^{37–46} Theoretical treatment argues that a *static disordered vortex solid* could be, dynamically, transformed to a *moving solid state* (that possibly retains crystalline order in some degree) under the influence of high driving forces.^{38–42} We believe that such a physical process could be related to the results presented here. As we apply high enough ac fields the force acting on vortices reduces the effective disorder and a moving vortex solid state is recovered in the regime between the $H_{\text{end point}}$ and the H_{irr} lines. This “healed” solid phase seems to exhibit, at least, the dynamic behavior of the ordered solid.²⁷ It should be natural then to assume that the possible reordering observed above the line $H_{\text{end point}}$ is due to the smoothing of static disorder by the combination of the increasing thermal energy and/or high driving forces. Such a dynamic process could not exist at arbitrarily high dc fields. Koshelev and Vinokur argued that the so-called “crystallization current,” needed for reordering the vortex solid, exceeds essentially the critical current and diverges as temperature approaches the melting point of the undistorted ideal lattice of vortices.³⁸ In our case, as we apply higher dc fields bulk pinning becomes dominant due to the increase of the effective static disorder.⁴ As a consequence, the critical current density increases rapidly and the driving force acting on vortices by the applied ac field never equals the “crystallization current.” So, above a characteristic point ($H \approx 3000$ Oe) we cannot recover the ordered state and an amorphous state is fully preserved up to the irreversibility line H_{irr} .

In order to investigate further the physical cause of the observed behavior in the regime of the SP, we performed ac permeability measurements for increasing and decreasing the temperature. Figure 7(a) depicts the variation of $\mu'(T)$ at various dc fields for a small ac field, $H_0 = 2.8$ Oe. The experimental procedure of these measurements is as following: under zero ac and dc fields, the superconductor is cooled to the desired temperature $T_{\text{min}} \approx 77.8$ K. Then we apply the ac and dc fields and measure during warming until T_c is ex-

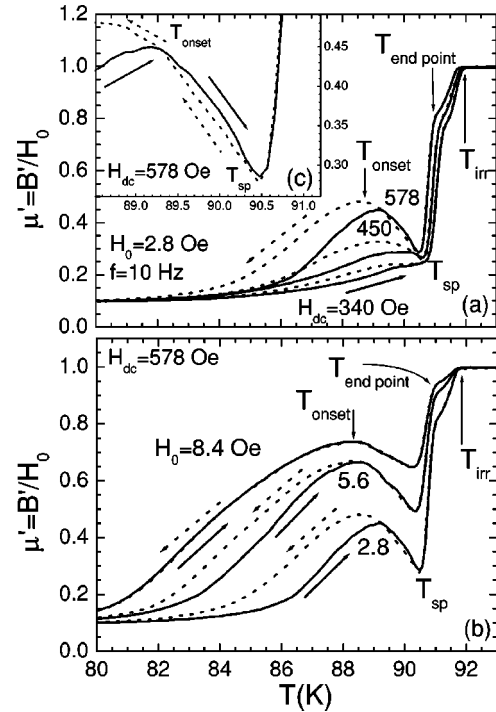


FIG. 7. Real part, $\mu' = B'/H_0$, of the local fundamental ac permeability as a function of temperature (a) at constant $H_0 = 2.8$ Oe and various dc fields, $H_{\text{dc}} = 340, 450,$ and 578 Oe and (b) at constant dc field, $H_{\text{dc}} = 578$ Oe, for various ac fields, $H_0 = 2.8, 5.6,$ and 8.4 Oe ($\mathbf{H}_{\text{dc}}, \mathbf{H}_{\text{ac}} \parallel c$). Inset (c) presents in detail the signal in the regime where the response is reversed. The solid (dashed) lines correspond to the increasing (decreasing) branches.

ceeded. The second part of the measurement is accomplished by measuring during decreasing the temperature, under the presence of the ac and dc fields. While the decreasing branches (dashed lines) coincide with the increasing ones (solid lines) in the temperature interval $T \geq T_{\text{sp}}$, pronounced hysteresis is observed in the regime below the OP of the SP. In the temperature regime $T_{\text{onset}} \leq T \leq T_{\text{sp}}$ minor hysteresis occurs when the applied ac field is low enough. As Fig. 7(c) resolves, *the decreasing branch is placed below the increasing one in the regime $T_{\text{onset}} \leq T \leq T_{\text{sp}}$* , but as we lower the temperature through the onset point, the opposite behavior is observed. This means that in the interval $T_{\text{onset}} \leq T \leq T_{\text{sp}}$ ($T \leq T_{\text{onset}}$) the field-cooled state of vortex matter possesses higher (lower) critical current J_c than the zero-field-cooled one. The behavior observed in the regime $T_{\text{onset}} \leq T \leq T_{\text{sp}}$ is consistent to the general requirements of an order-disorder transition^{43,45,46} (such a weak hysteretic effect probably cannot be observed in global measurements). On the other hand, the behavior observed below the OP is not compatible to the above-mentioned transformation.

Recently, Valenzuela and Bekkeris in a set of experiments studied the dynamics of vortex matter in the low-field regime of the SP.²⁷ Their experiments referred to twinned single crystals. To eliminate the influence of twin planes they tilted the applied fields from the c axis. By investigating different experimental procedures (regarding the application of the ac field), they concluded that, when an ac field is applied while

cooling the sample, the vortex solid is “healed.” This healed vortex state possesses lower critical current compared to the vortex solid which is produced by cooling in zero ac field. We observe the same behavior in our measurements in the temperature regime below the OP. So, we assume that the hysteretic behavior observed below the OP could be attributed to a dynamic rearrangement of a temporarily disordered vortex solid to a more ordered one. In contrast, in the regime between the OP and the SP where the order-disorder transition occurs, the field-cooled vortex solid is pinned more effectively than the zero-field-cooled state, even if we apply an ac field during the cooling process. In measurements performed for higher dc fields (not shown here) the decreasing branches are always placed below the increasing ones in the whole temperature regime $T \leq T_{sp}$. This result is a direct consequence of the enhancement of the effective quenched point disorder as we increase the magnetic field.⁴ Figure 7(b) reveals that, at constant dc field, $H_{dc} = 578$ Oe, the effect is more pronounced for small amplitudes of the ac field. As we apply higher ac field the effect is no more evident. This fact indicates that a high enough ac drive eliminates the dependence on the thermomagnetic history of vortex matter. Qualitatively, a similar behavior was recently observed for the $HgBa_2CuO_{4+\delta}$ superconductor.⁴⁶

Let us now discuss the possible influence (if any) of the geometrical/surface barriers in the low-field regime of our measurements. An edge barrier mechanism manifests itself in local measurements by enforcing special characteristics, such as the so-called “pinch-off field” (recognized in measurements, not only as a function of dc field, but also as a function of temperature) and negative values of the (local) permeability.¹⁹ For the case of an edge barrier, the decreasing branch is always placed *above* the increasing one (as in our case, see Fig. 7), in contrast to what is expected for the case

of an order-disorder transition. Of course, a pronounced contribution of an irreversibility mechanism of this type is expected only in bulk pinning free samples as recently was established for $Bi_2Sr_2CaCu_2O_8$ and $YBa_2Cu_3O_{7-\delta}$.^{19,47,48} In addition, in the high-temperature regime, close to T_c , our global SQUID magnetization loops exhibit distinguishable asymmetry (not shown here). This experimental observation cannot originate from a bulk pinning mechanism. To conclude, although we believe that bulk pinning is, undoubtedly, the dominant mechanism in this crystal, we cannot exclude a small contribution of an edge barrier in our measurements.

III. CONCLUSIONS

We presented local Hall ac permeability measurements for a $YBa_2Cu_3O_{7-\delta}$ detwinned, underdoped single crystal. The SP line H_{sp} does not terminate at the critical temperature but disappears at a characteristic point $(H, T) \approx (200 \text{ Oe}, 91.2 \text{ K})$. The onset H_{onset} and the end point $H_{end\ point}$ lines tend to T_c but could be detected until $(H, T) \approx (80 \text{ Oe}, 91.6 \text{ K})$. The end point $H_{end\ point}$ and irreversibility, H_{irr} lines practically coincide in the high-field regime, above a characteristic field $H \approx 3000$ Oe, while below this field they segregate. The observed behavior could be attributed to a reentrance of the quasiordered vortex state in the regime below the irreversibility line H_{irr} . Under this point of view, the H_{onset} and $H_{end\ point}$ lines are two parts of the same transition or crossover line from a Bragg glass to an amorphous solid. This composite line, smoothly, connects to the irreversibility line H_{irr} . Based on our experimental results we cannot conclude whether this process is of equilibrium character²⁶ or is a dynamically driven transition³⁸ as recently was theoretically proposed.

-
- ¹G. Blatter, M.V. Feigel'man, V.B. Geshkenbein, A.I. Larkin, and V.M. Vinokur, *Rev. Mod. Phys.* **66**, 1125 (1994).
²E.H. Brandt, *Rep. Prog. Phys.* **58**, 1465 (1995).
³T. Nattermann and S. Scheidl, *Adv. Phys.* **49**, 607 (2000).
⁴T. Giamarchi and P. Le Doussal, *Phys. Rev. B* **52**, 1242 (1995); **55**, 6577 (1997); *Phys. Rev. Lett.* **72**, 1530 (1994).
⁵D. Ertas and D.R. Nelson, *Physica C* **272**, 79 (1996).
⁶M.J.P. Gingras and D.A. Huse, *Phys. Rev. B* **53**, 15 193 (1996).
⁷A.E. Koshelev and V.M. Vinokur, *Phys. Rev. B* **57**, 8026 (1998).
⁸V. Vinokur, B. Khaykovich, E. Zeldov, M. Konczykowski, R.A. Doyle, and P.H. Kes, *Physica C* **295**, 209 (1998).
⁹J. Kierfeld, *Physica C* **300**, 171 (1998); J. Kierfeld and V. Vinokur, *Phys. Rev. B* **61**, R14 928 (2000); *Phys. Rev. Lett.* **85**, 4948 (2000).
¹⁰M.P.A. Fisher, *Phys. Rev. Lett.* **62**, 1415 (1989); D.S. Fisher, M.P.A. Fisher, and D.A. Huse, *Phys. Rev. B* **43**, 130 (1991).
¹¹D.R. Nelson, *Phys. Rev. Lett.* **60**, 1973 (1988).
¹²A. Houghton, R.A. Pelcovits, and A. Sudbo, *Phys. Rev. B* **40**, 6763 (1989).
¹³E.H. Brandt, *Phys. Rev. Lett.* **63**, 1106 (1989).
¹⁴L.I. Glazman and A.E. Koshelev, *Phys. Rev. B* **43**, 2835 (1991).
¹⁵K. Deligiannis, P.A.J. de Groot, M. Oussena, S. Pinfold, R. Langan, R. Gagnon, and L. Taillefer, *Phys. Rev. Lett.* **79**, 2121 (1997).
¹⁶S. Kokkaliaris, S.N. Gordeev, P.A.J. de Groot, R. Gagnon, L. Taillefer, P.F. Henry, and M.T. Weller, *Physica C* **320**, 161 (1999); S. Kokkaliaris, A.A. Zhukov, P.A.J. de Groot, R. Gagnon, L. Taillefer, and T. Wolf, *Phys. Rev. B* **61**, 3655 (2000).
¹⁷A.I. Rykov, S. Tajima, F.V. Kusmartsev, E.M. Forgan, and Ch. Simon, *Phys. Rev. B* **60**, 7601 (1999).
¹⁸A.A. Zhukov, H. Kupfer, G. Perkins, L.F. Cohen, A.D. Caplin, S.A. Klestov, H. Claus, V.I. Voronkova, T. Wolf, and H. Wuhl, *Phys. Rev. B* **51**, 12 704 (1995); H. Kupfer, Th. Wolf, C. Lessing, A.A. Zhukov, X. Lancon, R. Meier-Hirmer, W. Schauer, and H. Wuhl, *ibid.* **58**, 2886 (1998); H. Kupfer, Th. Wolf, R. Meier-Hirmer, and A.A. Zhukov, *Physica C* **332**, 80 (2000).
¹⁹M. Pissas and D. Stamopoulos, *Phys. Rev. B* **64**, 134510 (2001).
²⁰M. Pissas, E. Moraitakis, G. Kallias, and A. Bondarenko, *Phys. Rev. B* **62**, 1446 (2000).
²¹M. Pissas, E. Moraitakis, G. Kallias, and A. Bondarenko, *Physica C* **341**, 1331 (2000).
²²D. Giller, A. Shaulov, Y. Yeshurun, and J. Giapintzakis, *Phys. Rev. B* **60**, 106 (1999).

- ²³Y. Radzyner, S.B. Roy, D. Giller, Y. Wolfus, A. Shaulov, P. Chad-dah, and Y. Yeshurun, Phys. Rev. B **61**, 14 362 (2000).
- ²⁴B. Khaykovich, E. Zeldov, D. Majer, T.W. Li, P.H. Kes, and M. Konczykowski, Phys. Rev. Lett. **76**, 2555 (1996); B. Khaykov-ich, M. Konczykowski, E. Zeldov, R.A. Doyle, D. Majer, P.H. Kes, and T.W. Li, Phys. Rev. B **56**, 517 (1997).
- ²⁵D. Stamopoulos and M. Pissas, Supercond. Sci. Technol. **14**, 844 (2001).
- ²⁶G.P. Mikitik and E.H. Brandt, Phys. Rev. B **64**, 184514 (2001).
- ²⁷S.O. Valenzuela and V. Bekeris, Phys. Rev. Lett. **84**, 4200 (2000); **86**, 504 (2001); S.O. Valenzuela, B. Maiorov, E. Osquiguil, and V. Bekeris, Phys. Rev. B **65**, 060504 (2002).
- ²⁸D. Pal, D. Dasgupta, B.K. Sarma, S. Bhattacharya, S. Ramakrish-nan, and A.K. Grover, Phys. Rev. B **62**, 6699 (2000).
- ²⁹A.A. Zhukov, A.A. Bush, I.V. Gladyshev, S.N. Gordeev, and V.V. Moshchalkov, Z. Phys. B: Condens. Matter **78**, 195 (1990).
- ³⁰B. Billon, M. Charalambous, J. Chaussy, R. Koch, and R. Liang, Phys. Rev. B **55**, 14 753 (1997).
- ³¹T. Ishida, K. Okuda, and H. Asaoka, Phys. Rev. B **56**, 5128 (1997); T. Ishida, K. Okuda, A.I. Rykov, S. Tajima, and I. Terasaki, *ibid.* **58**, 5222 (1998).
- ³²D. Bracanovic, S.N. Gordeev, S. Pinfold, R. Langan, M. Oussena, P.A.J. de Groot, R. Gagnon, and L. Taillefer, Physica C **296**, 1 (1998); S.N. Gordeev, D. Bracanovic, A.P. Rassau, P.A.J. de Groot, R. Gagnon and L. Taillefer, Phys. Rev. B **57**, 645 (1998).
- ³³J. Shi, X.S. Ling, R. Liang, D.A. Bonn, and W.N. Hardy, Phys. Rev. B **60**, 12 593 (1999).
- ³⁴H. Safar, P.L. Gammel, D.A. Huse, D.J. Bishop, J.P. Rice, and D.M. Ginsberg, Phys. Rev. Lett. **69**, 824 (1992).
- ³⁵M. Charalambous, J. Chaussy, P. Lejay, and V. Vinokur, Phys. Rev. Lett. **71**, 436 (1993).
- ³⁶W.K. Kwok, S. Fleshler, U. Welp, V.M. Vinokur, J. Downey, G.W. Crabtree, and M.M. Miller, Phys. Rev. Lett. **69**, 3370 (1992); W.K. Kwok, J. Fendrich, U. Welp, S. Fleshler, J. Downey, and G.W. Crabtree, *ibid.* **72**, 1088 (1994); W.K. Kwok, J. Fendrich, S. Fleshler, U. Welp, J. Downey, and G.W. Crabtree, *ibid.* **72**, 1092 (1994); W.K. Kwok, J. Fendrich, C.J. van der Beek, and G.W. Crabtree, *ibid.* **73**, 2614 (1994).
- ³⁷J.A. Fendrich, U. Welp, W.K. Kwok, A.E. Koshelev, G.W. Crab-tree, and B.W. Veal, Phys. Rev. Lett. **77**, 2073 (1996); G.W. Crabtree, W.K. Kwok, U. Welp, J.A. Fendrich, and B.W. Veal, J. Low Temp. Phys. **105**, 1073 (1996).
- ³⁸A.E. Koshelev and V.M. Vinokur, Phys. Rev. Lett. **73**, 3580 (1994).
- ³⁹T. Giamarchi and P. Le Doussal, Phys. Rev. Lett. **76**, 3408 (1996).
- ⁴⁰L. Balents, M.C. Marchetti, and L. Radzihovsky, Phys. Rev. B **57**, 7705 (1998).
- ⁴¹C.J. Olson, C. Reichhardt, and F. Nori, Phys. Rev. Lett. **81**, 3757 (1998).
- ⁴²A. van Otterlo, R.T. Scalettar, G.T. Zimnyi, R. Olsson, A. Petrean, W. Kwok, and V. Vinokur, Phys. Rev. Lett. **84**, 2493 (2000).
- ⁴³W. Henderson, E.Y. Andrei, M.J. Higgins, and S. Bhattacharya, Phys. Rev. Lett. **77**, 2077 (1996); W. Henderson, E.Y. Andrei, and M.J. Higgins, *ibid.* **81**, 2352 (1998); Z.L. Xiao, E.Y. Andrei, and M.L. Higgins, *ibid.* **83**, 1664 (1999).
- ⁴⁴N.R. Dilley, J. Hermann, S.H. Han, and M.B. Maple, Phys. Rev. B **56**, 2379 (1997).
- ⁴⁵X.S. Ling, J.E. Berger, and D.E. Proper, Phys. Rev. B **57**, 3249 (1998).
- ⁴⁶D. Stamopoulos and M. Pissas, Phys. Rev. B **65**, 134524 (2002).
- ⁴⁷N. Morozov, E. Zeldov, D. Majer, and B. Khaykovich, Phys. Rev. Lett. **76**, 138 (1996).
- ⁴⁸N. Morozov, E. Zeldov, M. Konczykowski, and R.A. Doyle, Physica C **291**, 113 (1997).